J|A|C|S COMMUNICATIONS

Published on Web 09/28/2010

Platinum-Monolayer Shell on $AuNi_{0.5}Fe$ Nanoparticle Core Electrocatalyst with High Activity and Stability for the Oxygen Reduction Reaction

Kuanping Gong, Dong Su, and Radoslav R. Adzic*

Brookhaven National Laboratory, Upton, New York 11973

Received July 19, 2010; E-mail: Adzic@bnl.gov

Abstract: We describe a simple method for preparing multimetallic nanoparticles by in situ decomposition of the corresponding Prussian blue analogue, which is adsorbed on carbon black. The example involves the $AuNi_{0.5}Fe$ core of the $Pt_{ML}/Au_1Ni_{0.5}Fe$ core−shell electrocatalyst for the oxygen reduction reaction. The core contains 3−5 surface atomic layers of Au, which play an essential role in determining the activity and stability of the catalyst. The $Pt_{ML}/AuNi_{0.5}Fe$ electrocatalyst exhibited Pt mass and specific activities of 1.38 A/mg_{Pt} and 1.12 $\times$ 10^{-3} A/cm^2_{Pt}, respectively, both of which are several times higher than those of commercial Pt/C catalysts. Its all-noble-metal mass activity (0.18 $A/mg_{Pt,Au}$) is higher than or comparable to those of commercial samples. Stability tests showed an insignificant loss in activity after 15 000 triangular-potential cycles. We ascribe the high activity and stability of the $Pt_{ML}/AuNi_{0.5}Fe$ electrocatalyst to its hierarchical structural properties, the Pt-core interaction, and the high electrochemical stability of the gold shell that precludes exposure to the electrolyte of the relatively active inner-core materials.

Syntheses of stable multimetallic nanoparticles have been the subject of intensive research in electrocatalysis of the oxygen reduction reaction (ORR) because they have superior properties compared with their single-element counterparts.[1−6] Platinum monolayer (Pt_{ML}) electrocatalysts, comprising a Pt monolayer deposited on a metallic nanoparticle core, are one of the most promising catalytic materials for the ORR.[5] These electrocatalysts often have mass activities that are more than 1 order of magnitude higher than those of conventional all-Pt electrocatalysts. Like their activity, platinum monolayers' stability is determined by the nature of the support, its composition, and its structure. For most of the Pt_{ML} electrocatalysts developed to date, further improvement in the stability of the supporting cores and the core−shell interaction is desirable.

Here we report the synthesis of core−shell $AuNi_{0.5}Fe$ nanoparticles consisting of 3−5 atomic layers of Au on the three-element alloy core and demonstrate their essential role in realizing high overall performance of supported Pt for the ORR in $HClO_4$ solutions. Since Au and Ni or Fe atoms have a big miscibility gap and significantly different rates of nucleation and growth,[7] their alloyed or core−shell structures have been prepared by only a few synthetic procedures. Exemplary methods include low-energy cluster beam deposition,[8] reverse microemulsion reaction,[9] redox transmetalation,[10] and successive or simultaneous reduction of the solid metal precursors.[2,11] These methods require special surfactants, organic solvents, or harsh conditions.

In this communication, we report on a straightforward method involving in situ decomposition of $AuNi_{0.5}Fe(CN)_6$ for the preparation of $AuNi_{0.5}Fe$ nanoparticles, which can act as a new, improved support for Pt_{ML} electrocatalysts that features a clean surface, controlled composition, and a favorable Pt−core interaction.

In a typical synthesis, equivalent amounts of $K_4Fe(CN)_6$, $AuCl_3$, and $NiCl_2 \cdot 6H_2O$ were mixed with carbon black to form $AuNi_{0.5}Fe(CN)_6$, a Prussian blue analogue. The formed $AuNi_{0.5}Fe(CN)_6$ in situ produced $AuNi_{0.5}Fe$ nanoparticles on carbon (i.e., $AuNi_{0.5}Fe$/C) upon chemical decomposition at 500 °C under a reducing atmosphere [see the Supporting Information (SI)]. The size of the equipment (e.g., mortar and furnace) used to produce $AuNi_{0.5}Fe(CN)_6$/C and $AuNi_{0.5}Fe$/C determined the amount of the catalyst produced. Prussian blue analogues are polynuclear hexacyanometalate structures having the representative chemical formula, $M_x[M'(CN)_6]_y$, where both M and M′ are transition metals; their structures are generally of spatial symmetry in both the metal sites and the entire crystalline lattice.[12,13] By forming $AuNi_{0.5}Fe(CN)_6$, we "forced" the three different ions to mix with each other, thereby giving a homogeneous spatial configuration at the atomic level. Furthermore, the formation of $AuNi_{0.5}Fe(CN)_6$ appeared to result in energy transfer to Fe(II) sites of $Fe(CN)_6^{4-}$ from Au(III) through the cyanide bridging group (see the SI), which is in good agreement with the properties of the Prussian blue analogues reported

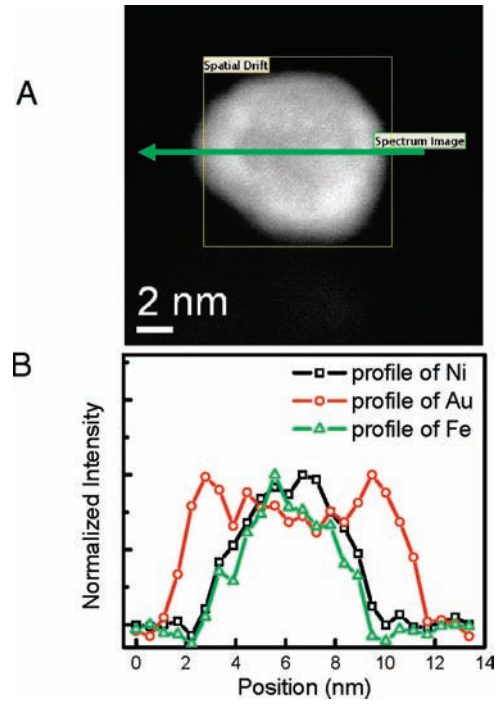

Figure 1. (A) HAADF-STEM image of a single $AuNi_{0.5}Fe$ nanoparticle on carbon black. The arrow indicates the electron probe's scanning direction. Two respective scans were taken at the same position, one with the energy range of Ni and Fe and the other with that of Au. (B) EELS line-scan profiles of Ni, Fe, and Au showing a core−shell structure with a shell thickness of ~1.0 nm.

10.1021/ja1063873

previously.[13] These features ruled out differences between the metal moieties in the nucleation kinetics, a crucial factor in preparing multimetallic nanostructures. This is especially the case for those multimetallic nanoparticles whose elemental components have significantly different reduction potentials. Consequently, the thermal decomposition of $AuNi_{0.5}Fe(CN)_6$ at a high temperature was likely to yield multimetallic nanoparticles that are homogeneous at the atomic level. Moreover, because of the different surface segregation energies, the Au phase can partially segregate from NiFe and move to the surface upon cooling of the pyrolyzed sample from the decomposition temperature, inducing the formation of a core−shell structure.[14]

A high-angle annular dark-field scanning transmission electron microscopy (HAADF-STEM) image of the prepared sample showed nanoparticles with diamters of ∼8 nm on carbon black; the elemental components of the individual nanoparticles were identified to be Au, Ni, and Fe by electron energy loss spectroscopy (EELS) (Figure S4 in the SI). The elemental components and composition

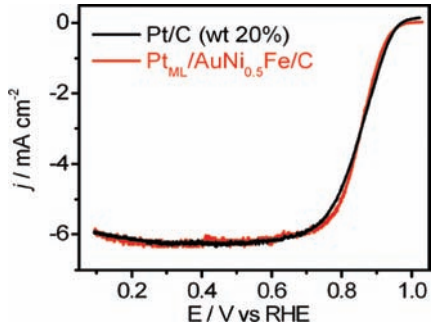

Figure 2. RDE polarization curves of $Pt_{ML}/AuNi_{0.5}Fe/C$ and Pt/C (20 wt %, E-TEK) electrocatalysts in high-purity oxygen-saturated 0.1 M $HClO_4$. Conditions: scan rate, 10 mV s^{-1}; rotation speed, 1600 rpm; Pt loading, 1.5 $\mu g/cm^2$ ($Pt_{ML}/AuNi_{0.5}Fe/C$) or 10.2 $\mu g/cm^2$ (Pt/C). The current density is expressed with respect to the geometric surface area.

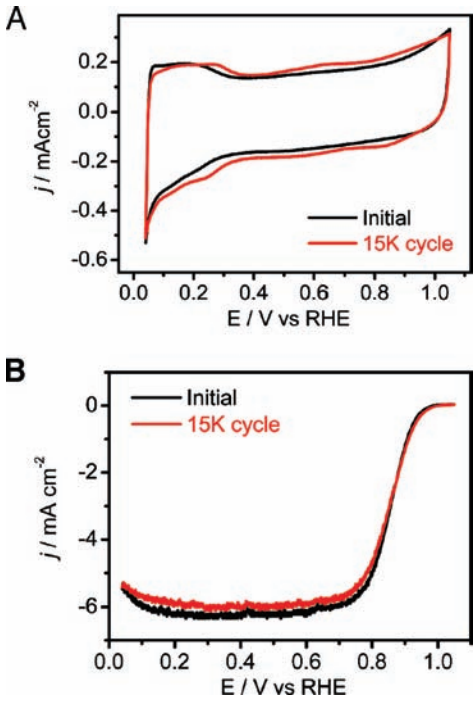

Figure 3. (A) CVs and (B) RDE polarization curves for $Pt_{ML}/AuNi_{0.5}Fe/C$ before and after 15 000 cycles of sweeping the potential between 0.6 and 1.0 V at 50 mV s^{-1}. The current density is expressed with respect to the geometric surface area.

were further verified with inductively coupled plasma−atomic emission spectrometry (ICP−AES) analyses: we obtained ∼25.0 wt % $AuNi_{0.5}Fe$ with an approximate atomic ratio of 1:0.5:1 on carbon black. This is in excellent agreement with the amount of the precursors used in this synthesis, suggesting good efficiency of the synthetic method.

Figure 1 shows a high-magnification HAADF-STEM image of a $AuNi_{0.5}Fe/C$ nanoparticle, along with the corresponding linear-scan EELS spectrum, confirming the core−shell structure. From these data, we infer that the core−shell nanoparticles are composed of an Au shell with a thickness of 1.0 nm and a trimetallic alloy core of Au, Ni, and Fe. On the basis of the Au atomic layer spacing of ∼0.24 nm, the shell of the $AuNi_{0.5}Fe$ nanoparticles apparently consists of 3−5 Au atomic layers.

Figure 2 shows rotating disk electrode (RDE) polarization curves of the $Pt_{ML}/AuNi_{0.5}Fe/C$ and Pt/C electrocatalysts, which demonstrate the comparable apparent activities of the two electrocatalysts for the ORR. As expected, for the $Pt_{ML}/AuNi_{0.5}Fe/C$ electrocatalyst, the Pt mass and specific activities were improved 5- to 7-fold in comparison with the Pt/C electrocatalyst (Table 1). It is important to note that the noble-metal mass activity of $Pt_{ML}/AuNi_{0.5}Fe/C$ is 0.18 A/mg, which is much higher than those of its all-Pt counterparts having a particle size of 8 nm. This mass activity, if normalized by the price of platinum, is even higher than that of the most active 3.5 nm Pt electrocatalyst (Table S1 in the SI). Such comparisons reveal that underpinning Au with Ni and Fe atoms is essential for the formulation of an excellent support for the Pt_{ML} electrocatalyst with high activity for the ORR.

Table 1. Comparison of the ORR Kinetics on $Pt_{ML}/AuNi_{0.5}Fe/C$ and Pt/C Electrocatalysts[a]

	$E_{1/2}$ (V vs RHE)	specific activity (10^{-3} A/cm^2_{Pt})[b]	mass activity (A/mg_{Pt})[c]	mass activity (A/mg_{Pt+Au})[d]
$Pt_{ML}/AuNi_{0.5}Fe/C$	858	1.12	1.38	0.18
Pt/C	852	0.22	0.19	0.19

[a] The current at 900 mV in Figure 2 was used to calculate the kinetic current based on the Koutecký−Levich equation.[15] [b] The Pt electrochemical surface areas were 0.34 and 1.73 cm^2 for the $Pt_{ML}/AuNi_{0.5}Fe/C$ and Pt/C electrocatalysts, respectively. [c] Mass activity in terms of platinum mass. [d] Mass activity in terms of total mass of noble metal.

Platinum binds oxygen a little too strongly, so the removal of the oxygen species to refresh the active site limits the overall ORR kinetics. The Pt−O bond becomes much stronger for a Pt monolayer on gold because their mismatch in lattice constant causes platinum to be less coordinated.[5] This negative ligand effect of gold on the platinum monolayer can be mitigated in the $AuNi_{0.5}Fe$ particles by the lattice contraction of Au itself as a consequence of alloying of Au with Ni and Fe (Figure S3). On the other hand, as Ni and Fe have relatively high Fermi levels (i.e., low standard redox potentials[16]), they can enable the intake of their 3d electrons into Au, causing Au to have a downward shift of the d-band center relative to the Fermi level. Therefore, the electronic effect of Ni and Fe atoms on Au in the $AuNi_{0.5}Fe$ particles might weaken the depletion of the d-band electrons of platinum that has been reported for $Pt_{ML}/Au(111)$,[5] realizing a relatively favorable (moderate) Pt−O binding strength. Overall, the fine-tuned d-band center and lattice constant of the Au shell can most likely account for the observed high specific activity of the $Pt_{ML}/AuNi_{0.5}Fe/C$ electrocatalyst for the ORR.

Our choice of the $AuNi_{0.5}Fe$ nanoparticle as a Pt_{ML} support was also aimed at achieving high stability, which is of vital importance in developing a real-world electrocatalyst. We adopted the new DOE protocol[17] to study the stability of the $Pt_{ML}/AuNi_{0.5}Fe/C$ electro-

catalyst. Figure 3A shows cyclic voltammograms (CVs) of Pt_{ML}/$AuNi_{0.5}Fe$/C before and after the stability test. We observed an insignificant loss in the electrochemical surface area of the electrocatalyst, indicating robust mechanical stability of Pt_{ML} at the $AuNi_{0.5}Fe$ surface. It is noteworthy that after the stability test, a new couple of redox peaks centered at 0.55 V, due mainly to the oxidation of carbon black at high potentials, was seen. Likewise, the ORR activity of the $Pt_{ML}/AuNi_{0.5}Fe$/C remained almost unchanged, as evidenced by the nearly overlapped RDE voltammograms recorded before and after the stability test (Figure 3B). Our previous work reported the stabilization of Pt nanoparticles with Au clusters because gold can elevate the oxidation potential of platinum;[6] the same origin of the stability might be true for the case of $Pt_{ML}/AuNi_{0.5}Fe$/C, with long-term durability in both mechanical properties and electrocatalytic activity. Indeed, the oxidation of platinum on the $Pt_{ML}/AuNi_{0.5}Fe$/C electrocatalyst commenced at a potential of 0.85 V (black curve in Figure 3A), which is 0.15 V higher than the counterpart oxidation potential on the Pt/C.[6]

To summarize, we have developed a new method involving in situ decomposition of a Prussian blue analogue for preparing $AuNi_{0.5}Fe$ nanoparticles as a new support for Pt_{ML} in a controllable manner. While the underpinning Ni and Fe atoms modified the Pt−core interaction, the gold shell precluded exposure of the relatively active inner core to the electrolyte, resulting in significantly improved activity and stability of the $Pt_{ML}/AuNi_{0.5}Fe$ electrocatalyst for the ORR at reduced costs.

Acknowledgment. This work was supported by the U.S. Department of Energy, Divisions of Chemical and Material Sciences, under Contract DE-AC02-98CH10886.

Supporting Information Available: Synthesis conditions; experimental procedures; XRD and TEM analyses of the nanoparticles; ORR activities of carbon-supported Pt particles of various sizes; and CVs of the $AuNi_{0.5}Fe(CN)_6$/C electrocatalyst. This material is available free of charge via the Internet at http://pubs.acs.org.

References

(1) Ferrando, R.; Jellinek, J.; Johnston, R. L. *Chem. Rev.* **2008**, *108*, 845–910.
(2) Fernández, J. L.; Raghuveer, V.; Manthirm, A.; Bard, A. L. *J. Am. Chem. Soc.* **2005**, *127*, 13100–13101.
(3) Mayrhofer, K. J. J.; Juhart, V.; Hartl, K.; Hanzlik, M.; Arenz, M. *Angew. Chem., Int. Ed.* **2009**, *48*, 3529–3531.
(4) Stamenkovic, V.; Mun, B. S.; Mayrhofer, K. J. J.; Ross, P. N.; Markovic, N. M.; Rossmeisl, J.; Greeley, J.; Nørskov, J. K. *Angew. Chem., Int. Ed.* **2006**, *45*, 2897–2901.
(5) Adzic, R. R.; Zhang, J.; Sasaki, K.; Vukmirovic, M. B.; Shao, M.; Wang, J. X.; Nilekar, A. U.; Mavrikakis, M.; Valerio, J. A.; Uribe, F. *Top Catal.* **2007**, *46*, 249–262, and references cited therein.
(6) Zhang, J.; Sasaki, K.; Sutter, E.; Adzic, R. R. *Science* **2007**, *315*, 220–222.
(7) Clinton, J. R.; Tyler, E. H.; Luo, H. L. *J. Phys. F: Met. Phys.* **1974**, *4*, 1162–1169.
(8) Rousset, J. L.; Cadete Santos Aires, F. J.; Sekhar, B. R.; Mélinon, P.; Prevel, B.; Pellarin, M. *J. Phys. Chem. B* **2000**, *104*, 5430–5435.
(9) Chen, D.; Li, J.; Shi, C.; Du, X.; Zhao, N.; Sheng, J.; Liu, S. *Chem. Mater.* **2007**, *19*, 3399–3405.
(10) Lee, W. R.; Kim, M. G.; Choi, J. R.; Park, J.; Ko, S. J.; Oh, S. J.; Cheon, J. *J. Am. Chem. Soc.* **2005**, *127*, 16090–16097.
(11) Shao, M.; Sasaki, K.; Adzic, R. R. *J. Am. Chem. Soc.* **2006**, *128*, 7408–7409.
(12) Kahn, O. *Nature* **1995**, *378*, 667.
(13) Mallah, T.; Thiébaut, S.; Verdaguer, M.; Veillet, P. *Science* **1993**, *262*, 1554–1557.
(14) Molenbroek, A. M.; Nørskov, J. K. *J. Phys. Chem. B* **2001**, *105*, 5450–5458.
(15) Bard, A. J.; Faulkner, L. R. *Electrochemical Methods: Fundamentals and Applications*, 2nd ed.; Wiley: New York, 2001.
(16) Charlot, G. *Oxidation−Reduction Potentials*; Pergamon Press: London, 1958.
(17) *Cell Component Accelerated Stress Test Protocols for PEM Fuel Cells*; U.S. Department of Energy: Washington, DC, 2008; Table 1.

JA1063873